International Journal of Astronomy and Astrophysics, 2018, 8, 68-78
http://www.scirp.org/journal/ijaa
ISSN Online: 2161-4725
ISSN Print: 2161-4717

# Mass of the Universe and the Redshift

**Rajendra P. Gupta**

Macronix Research Corporation, Ottawa, Canada
Email: sonice810@gmail.com, rajendra gupta

**How to cite this paper:** Gupta, R.P. (2018) Mass of the Universe and the Redshift. *International Journal of Astronomy and Astrophysics*, **8**, 68-78.
https://doi.org/10.4236/ijaa.2018.81005

**Received:** January 5, 2018
**Accepted:** March 12, 2018
**Published:** March 15, 2018



## Abstract

Cosmological redshift is commonly attributed to the continuous expansion of the universe starting from the Big-Bang. However, expansion models require simplifying assumptions and multiple parameters to get acceptable fit to the observed data. Here we consider the redshift to be a hybrid of two effects: recession of distant galaxies due to expansion of the universe, and resistance to light propagation due to cosmic drag. The weight factor determining the contribution of the two effects is the only parameter that is needed to fit the observed data. The cosmic drag considered phenomenologically yields mass of the universe ≈ $2 \times 10^{53}$ kg. This implicitly suggests that the mass of the whole universe is causing the cosmic drag. The databases of extragalactic objects containing redshift $z$ and distance modulus $\mu$ of galaxies up to $z$ = 8.26 resulted in an excellent fit to the model. Also, the weight factor $w_D$ for expansion effect contribution to $\mu$ obtained from the data sets containing progressively higher values of $\mu$ can be nicely fitted with $w_D(\mu) = 0.198\sin(0.4159\mu + 2.049) + 0.2418\sin(0.6768\mu + 5.15)$.

## Keywords

Redshift, Expanding Universe, Mach Effect, Cosmic Drag, Cosmological Constant

## 1. Introduction

Alternative explanations to Doppler effect, or expansion of the universe, for observed redshift of luminous objects in distant galaxies, such as tired light models, have never been taken seriously since it was first offered by Zwicky in 1929 [1]. There are many studies that show that expanding universe approach has certain problems, such as requiring simplifying assumptions and multiple parameters to get acceptable fit to the observed data. Geller and Peebles [2] have studied the tired-light static universe concept against the expanding universe concept. LaViolette [3] has shown that the tired-light model provides a better fit to the observed data without requiring the ad hoc introduction of assumptions about rapid galaxy evolution. Ghosh [4] has introduced a velocity dependent 'inertial induction' model as a possible mechanism for explaining the redshift in a quasi-static infinite universe. More recently, Marosi [5], Traunmuller [6], Orlov and Raikov [7], and others have shown that the static or slowly expanding universe models are viable alternatives to the standard ΛCDM models. López-Corredoira [8] in his most recent publication has critically analysed static and expansion models and established that both the approaches have unexplained gaps and arbitrariness.

The mechanism that leads to the loss of energy in tired light models has not been made clear in most of the studies although Compton scattering, or like models, have been cursorily suggested. The most used form of the tired light approach takes an exponential increase in photon wavelength with distance traveled:

$$\lambda_o = \lambda_e \mathrm{e}^{\frac{d}{R_o}}, \tag{1}$$

where $\lambda_o$ is the observed wavelength of the photon at distance $d$ from the source of emission, $\lambda_e$ is the wavelength of the photon at the source of light and $R_o$ is a constant that characterises the effect of the cause of the increase in wavelength whatever that may be.

The focus here is to derive Equation (1) from a simple model of resistance of the fields in space to the propagation of photons (and possibly other particles), similar to that of the propagation of a particle through a resistive field of a fluid in fluid dynamics

## 2. Cosmic Drag Model

In fluid dynamics, the particle ceases to accelerate when the applied force on a particle F equals fluid's resistance or drag:

$$F = \frac{1}{2}\rho v^2 A C_d. \tag{2}$$

Here $\rho$ is the density of the fluid through which the particle is propagating, $v$ is the particle velocity, $A$ is the particle area and $C_d$ is the fluids drag coefficient. Now this force $F$ may also be written as $-\frac{\mathrm{d}E}{\mathrm{d}x}$ where $\mathrm{d}E$ is the energy used up in moving the particle a distance $\mathrm{d}x$ in the fluid.

$$-\frac{\mathrm{d}E}{\mathrm{d}x} = \frac{1}{2}\rho v^2 A C_d. \tag{3}$$

Inspired by this equation, in our phenomenological cosmic drag model for a photon traveling through space, we write as follows:

$E = h\nu$, with $h$ as Planck's constant and $\nu$ as photon frequency,

$AC_d$ is assumed to be proportional to the energy $E$,

$\rho$ is a constant related to the entity causing the drag,

$v = c$, the speed of light.

We may then write:

$$-\frac{\mathrm{d}(h\nu)}{\mathrm{d}x} = \frac{(h\nu)c^2}{\kappa}. \tag{4}$$

Here $\kappa$ is a constant that captures $1/2\rho$ and the proportionality constant that relates $E$ to $AC_d$, thus representing the resistive properties of the cosmic drag fields on the photon. Integrating Equation (4) over distance $d$ from the photon emission point to the photon observation point, we have:

$$\ln\left(\frac{\nu_e}{\nu_o}\right) = \frac{c^2 d}{\kappa}, \tag{5}$$

or

$$\ln\left(\frac{\lambda_o}{\lambda_e}\right) = \frac{c^2 d}{\kappa}, \tag{6}$$

or

$$\frac{\lambda_o}{\lambda_e} = \mathrm{e}^{\frac{c^2 d}{\kappa}}. \tag{7}$$

Here, $\nu_e$ and $\nu_o$ are respectively the emitted and observed photon frequencies and $\lambda\nu = c$. Now, since the redshift is defined as $z = \frac{\lambda_o}{\lambda_e} - 1$, we may write Equation (7):

$$z + 1 = \mathrm{e}^{\frac{c^2 d}{\kappa}}, \tag{8}$$

or

$$\ln(1+z) = \frac{c^2 d}{\kappa} \tag{9}$$

The constant $\kappa$ can be determined from the small redshift limit of Equation (9) by appealing to the Hubble law. The law may be written for small $z$ as $cz = H_o d$, where $H_o$ is Hubble constant and $d$ is the distance of a galaxy with small redshift. This allows us to write for small values of $z$

$$\ln(1+z) \approx z = \frac{c^3 z}{H_o \kappa}, \tag{10}$$

or

$$\kappa = \frac{c^3}{H_o}, \text{ and} \tag{11}$$

$$d = \left(\frac{c}{H_o}\right)\ln(1+z). \tag{12}$$

Taking $c = 3\times10^8\ \mathrm{m/s}$ and $H_o = 2\times10^{-18}/\mathrm{s}$ (= 70 km/s/Mpc), we get $\kappa = 1.35\times10^{43}\,\mathrm{m^3\cdot s^{-2}}$. Before we proceed further let us see if this constant has some cosmological meaning.

## 3. Mass of the Universe

Looking at Newton's gravitational constant $G_N$, we notice that its dimensions are $m^3 \cdot k^{-1} \cdot s^{-2}$ with a value of $6.674 \times 10^{-11}$. Thus on the dimensional ground,

$$\kappa = M_x G_N , \tag{13}$$

where $M_x$ is an unknown mass factor related to the propagation of light in the universe. This yields

$$M_x = \frac{c^3}{H_o G_N} = 2 \times 10^{53} \text{ kg} . \tag{14}$$

We can readily recognize this as the mass of the observable universe (Hoyle-Carvalho formula [9]); it is in the same range as estimated in several studies, e.g. Valev [10] and Ostriker *et al.* [11].

Substituting $\kappa$ from Equation (13) into Equation (4), we have,

$$-\frac{\mathrm{d}(h\nu)}{\mathrm{d}x} = \frac{(h\nu)c^2}{M_x G_N} . \tag{15}$$

This equation shows that the drag on the photon depends on the mass of the observable universe and thus it is a manifestation of Mach's Principle [12]. We may therefore call this redshift as due to Mach Effect.

## 4. Observed Data Analysis

We will now proceed to fit the observed redshift data using the Doppler effect (including expansion effect) based model and the Mach effect based model proposed here, to explore if one or the other gives a better fit, or perhaps both the effects are partially accountable for the observed redshift. The model we chose for the first type is that recently developed analytically by Mostaghel [13] assuming a flat universe expanding under a constant pressure and combining the first and second Friedmann equations. This model yields a good fit to the whole range of redshift that was available to him in late 2015 as follows:

1) A set of 557 SNe data with redshifts from $0.0152 \le z \le 1.4$ as compiled in the 2010 in the Union2 database [14];

2) A set of 394 extragalactic distances to 349 galaxies at redshifts $0.133 \le z \le 6.6$ as reported in 2008 NASA/IPAC's NED-4D database [15]; and

3) Data for three most distant recently confirmed galaxies [16] [17] [18], and a quasar [19] with $7 \le z \le 9$.

The distance modulus $\mu$ and the redshift $z$ are represented by Mostaghel [13] as

$$\mu = 5\log\left[R_o(1-a)K(z)\right] + 25, \tag{16}$$

where $a$ is the scale factor, $R_o = c/H_o$ is in mega parsecs, and $K(z)$ includes K-correction that corrects observation data for source luminosity, instrumental factors, and other factors. With $1-a = z/(1+z)$ and $K(z) = (1+z)^b$,

$$\mu = 5\log\left[R_o\left(z/(1+z)\right)(1+z)^b\right] + 25 . \tag{17}$$

Mostaghel fitted 1st set of data in Equation (17), and found $b = 5/3$. This equation was used to fit all the three sets of data showing a reasonably good fit. (It should be mentioned that we found for all the three data sets a better fit is obtained by using $b = 1.487$ and not by using $b = 5/3$). He used his analytically derived value of $H_o = 69.05398$ km/s/Mpc in Equation (17) as he found it to be very close to the average of the most recently reported value of the Hubble constant. He found $z - \mu$ plots using Equation (17) were in good agreement with $\Lambda$CDM model fit with the same data using the scale factor given by equation

$$1/a(z) = \int_0^z \left[ \Omega_m (1+z') + \Omega_A (1+z')^{-2} + \Omega_r (1+z')^2 + \Omega_k \right]^{-\frac{1}{2}} \mathrm{d}z' + 1, \quad (18)$$

with $H_o = 68.45 \pm 0.96$, $\Omega_A = 0.703 \pm 0.012$, $\Omega_{m0} = 0.297 \pm 0.012$, $\Omega_{r0} = 0$ and $\Omega_k = 0$. We there for used Equation (18) as representing the expansion model, *i.e.* the Doppler effect model.

Based on Equation (12) for Mach effect model, distance modulus may be written as

$$\mu = 5\log\left[ R_o \ln(1+z) K'(z) \right] + 25, \quad (19)$$

with $K'(z) = (1+z)^d$ is correction factor for Mach Effect and d is determined by fitting the observational data.

The observational data we chose for our study is only slightly different from Mostaghel's data discussed above. We took (a) a set of 580 SNe data with redshifts from $0.015 \le z \le 1.414$ as compiled in the 2010 in the Union2 database [14]; and (b) a set of 382 extragalactic redshifts $1.414 \le z \le 8.26$ as reported in the updated 2017 NASA/IPAC's NED-D database [15]. The plots fitted to determine $b$ and $d$ using non-linear regression analysis, presented in **Figure 1** show the fit of the two models with the low $z$ observed data set (a). **Figure 2** plots include both the data sets (a) and (b) for the fit. The first four rows of **Table 1** presents the values of $b$ and $d$ for both the cases along with their 95% confidence bounds, SSEs (sum of squares due to errors), R-squares, and RMSE (root mean square errors).

As the redshift may be partly due to Doppler effect and partly due to Mach effect, we also considered fitting the observed data with weight factors given to Equations (17) and (19) and determining the weight factors with nonlinear regression analysis. Thus, we may write

$$\mu = w5\log\left[ R_o \ln(1+z)(1+z)^d \right] + (1-w)5\log\left[ R_o \left( \frac{z}{1+z} \right) (1+z)^b \right] + 25, \quad (20)$$

where $w$ is the weight factor given to Equation (19) and $(1-w)$ to Equation (17); two weight factors must add up to 1 and $0 \le w \le 1$. Parameters $b$ and $d$ we tried in Equation (20) for determining $w$ are as follows: 1) determined from fitting data set (a), that is $b = 1.671$ and $d = 1.194$; 2) determined from fitting the combined dataset (a) and (b), that is $b = 1.487$ and $d = 1.042$; and 3)

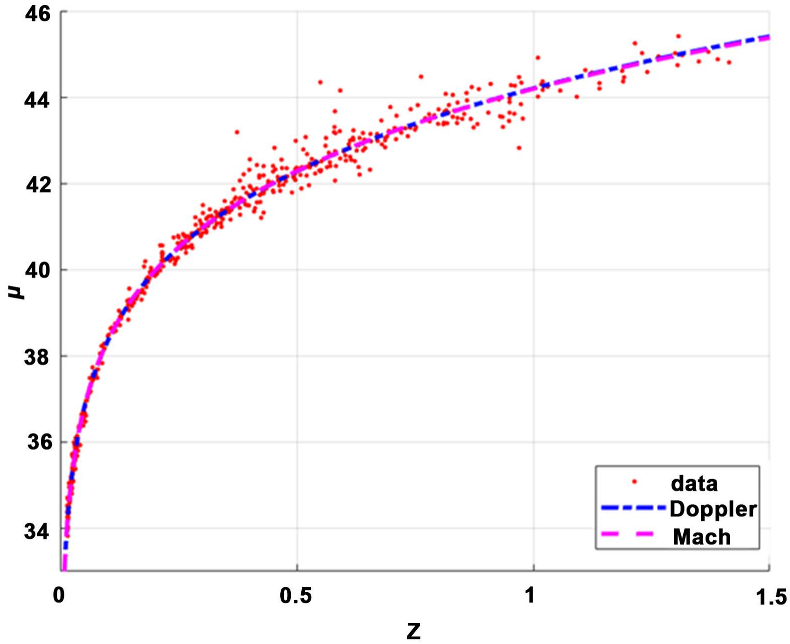


Figure 1. Observed data set $0 \le z \le 1.414$ fitted using Doppler Effect and Mach Effect based models.

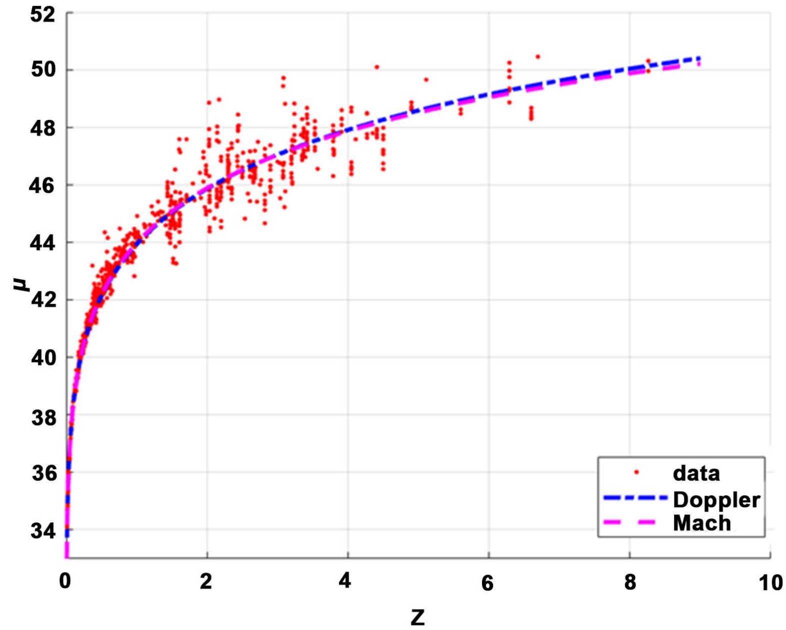


Figure 2. Observed data set $0 \le z \le 8.26$ fitted using Doppler Effect and Mach Effect based models.

$b = 2$ and $d = 1$. While parameters $b$ and $d$ may also be determined along with $w$ by fitting Equation (20) directly to the observed data, their variance becomes very high due to significant scatter in observed data. The fitted curves for the three cases are plotted in Figure 3 and corresponding weight factors $w$ along with their associated analysis parameters are given in Table 1 in the last three rows.

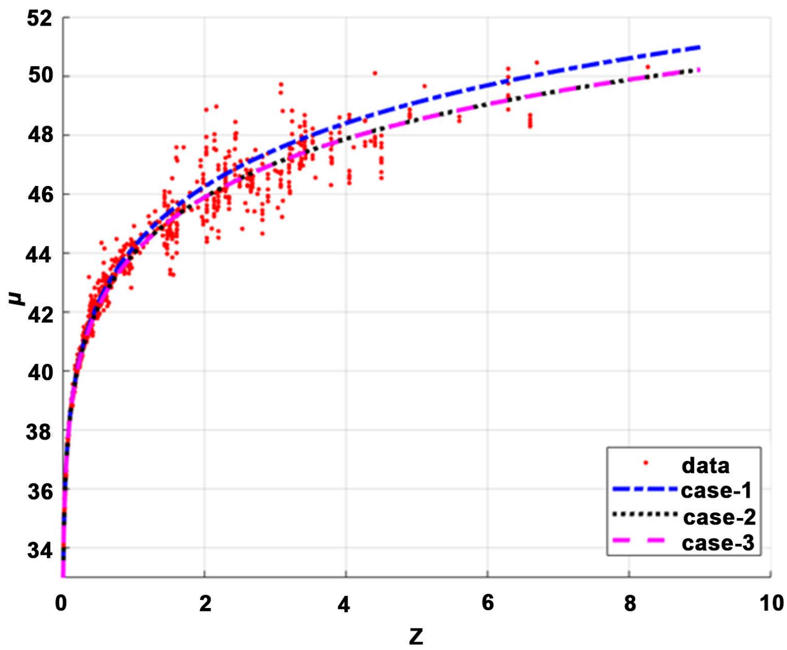


Figure 3. Observed data set $0 \le z \le 8.26$ fitted using a hybrid Doppler Effect and Mach Effect model with the weight factor for the two determined for the three cases: 1) $b = 1.671$ and $d = 1.194$; 2) $b = 1.487$ and $d = 1.042$; and 3) $b = 2$ and $d = 1$.

Table 1. Parameters obtained by fitting observed 2010 Union2 [14] and 2017 NASA/IPAC's NED-D database [15] to different models.

| Model reference | Data base | Data points | Model parameters | | 95% Confidence | | Goodness of fit | | |
|---|---|---|---|---|---|---|---|---|---|
| | | | Label | Value | | | SSE | R-Squared | RMSE |
| Doppler | *a* | 580 | *b* | 1.671 | 1.643 | 1.699 | 41.78 | 0.9929 | 0.2685 |
| Mach | *a* | 580 | *d* | 1.194 | 1.166 | 1.222 | 41.53 | 0.993 | 0.2678 |
| Doppler | *a* + *b* | 962 | *b* | 1.487 | 1.468 | 1.506 | 308.1 | 0.981 | 0.5666 |
| Mach | *a* + *b* | 962 | *d* | 1.042 | 1.023 | 1.06 | 302.2 | 0.9814 | 0.5611 |
| Case 1 | *a* + *b* | 962 | *w* | 1 | fixed at bound | | 381.9 | 0.9765 | 0.6304 |
| Case 2 | *a* + *b* | 962 | *w* | 1 | fixed at bound | | 302.2 | 0.9814 | 0.5608 |
| Case 3 | *a* + *b* | 962 | *w* | 0.9276 | 0.8936 | 0.9615 | 302.6 | 0.9814 | 0.5614 |

The weight factor appears to strongly favour Mach effect; $w \approx 1$. However due to logarithmic dependence of $\mu$ on *z*, *w* is also strongly dependent on parameters *b* and *d* of the $K(z)$ and $K'(z)$ factors, which in turn heavily depends on the *K*-correction. Here we are assuming that both the effects determine $\mu$ and *z*. Then, if we use the equation that only represent one effect, the exponent of $(1+z)^x$, with $x = b$ or *d*, has to take care of not only the *K*-correction, etc., but also for the other effect. Since *d* comes out to be up to 20% greater than 1, while *b* comes out to be up to 25% less than 2 (first four rows of Table 1), when using respective single effect equations, we believe taking $d = 1$

and $b=2$ for the first term and the second term respectively in Equation (20) may not be unreasonable to fit the data to determine *w*. This is why we have included case (3) for **Figure 3** and **Table 1** (last 3 rows). As can be seen case (3) gives almost identical result to case (2), which is better than case (1). We therefore decided to pursue further the case $d=1$ and $b=2$ by rewriting Equation (20) as follows:

$$\mu = 5(1-w_D)\log\left[R_o \ln(1+z)(1+z)\right] + 5w_D \log\left[R_o z(1+z)\right] + 25, \qquad (21)$$

where $w_D = (1-w)$ is now the Doppler effect weight factor. Sixteen data sets were created with progressively increasing value of $\mu$; say for $\mu = 40$ all the data up to $\mu = 40$ was included. For each data set, $w_D$ was determined by fitting the data using Equation (21). Resulting 16 data points $(\mu, w_D)$ were then fitted using a Gaussian function with the constraint that the factor $w_D$ satisfy the condition $0 \le w_D \le 1$. The plot is shown in **Figure 4**. We see a peak at $\mu = 42.06$ with $w_D = 0.325$ and FWHM of 3.38.

One problem with this plot we noticed is that the constraint $w_D = 0$ was hit 8 times. This suggests that $w_D$ has a tendency to go negative. When we removed the constraint on $w_D$, we got the data points that fitted beautifully a two term sine function (**Figure 5**):

$$w_D(\mu) = a_1 \sin(b_1\mu + c_1) + a_2 \sin(b_2\mu + c_2), \qquad (22)$$

with $a_1 = 0.198$, $b_1 = 0.4159$, $c_1 = 2.049$; $a_2 = 0.2418$, $b_1 = 0.6768$, $c_2 = 5.15$. This amounts to the Doppler effect contribution in Equation (21) to be negative in some regions and positive in others.

We may interpret the positive $w_D$ as indicative of the expansion of the universe and negative $w_D$ as contraction. As per **Figure 5**, the expansion of the universe starts at $\mu = 51.34$, peaks at $\mu = 49.89$, slows down up to $\mu = 48.24$, and then goes into contraction phase. The contraction peaks at $\mu = 46.38$, slows down up to $\mu = 44.80$, and then goes into expansion phase again; and so on. This fit may be extrapolated to higher values of $\mu$ using Equation (22) well beyond the maximum $\mu$ shown in the figure. This is shown in **Figure 6** from

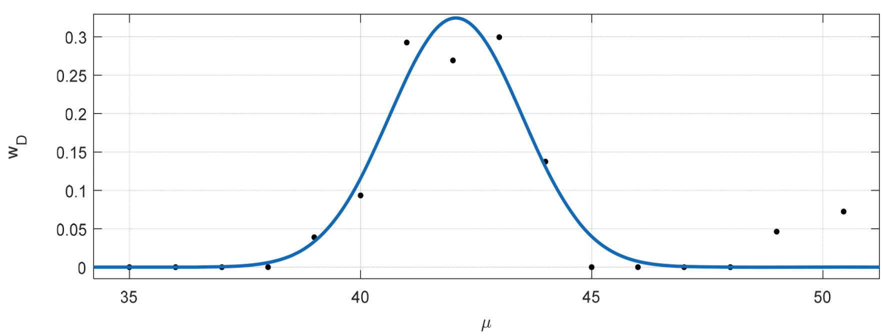


**Figure 4.** The Doppler effect weight factor $w_D$ bound to the condition $0 \le w_D \le 1$ and calculated using progressively incremental observed data base at 16 $\mu$ points shows a Gaussian behaviour. A peak is seen at $\mu = 42.06$ with $w_D = 0.325$ and FWHM of 3.38.

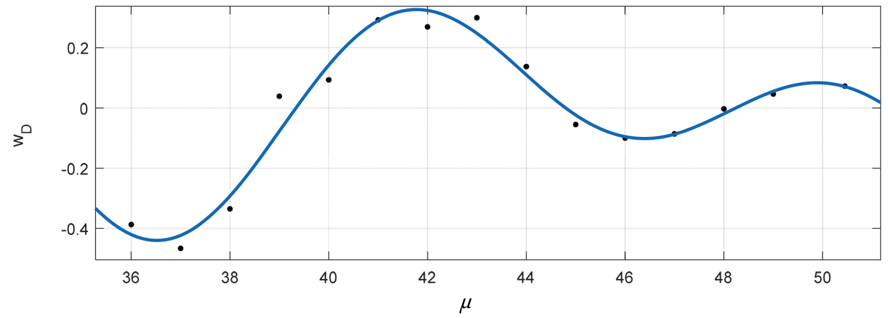


**Figure 5.** The Doppler effect weight factor $w_D$ liberated from the condition $0 \le w_D \le 1$ and calculated using progressively incremental observed data base at 15 $\mu$ points shows a good fit to a two term sine function $w_D(\mu) = 0.198\sin(0.4159\mu + 2.049) + 0.2418\sin(0.6768\mu + 5.15)$.

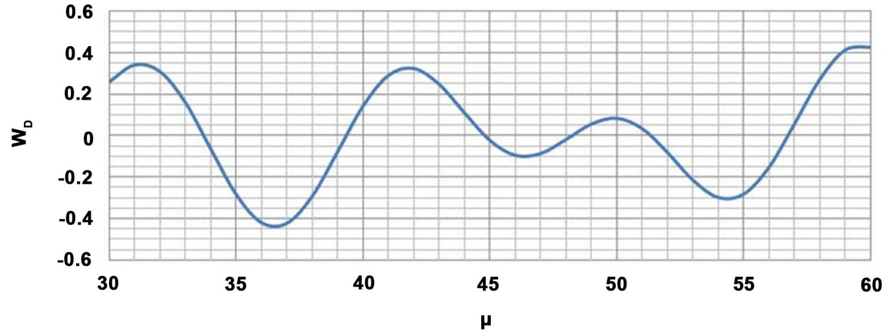


**Figure 6.** The Doppler effect weight factor $w_D$ plotted from $\mu = 30$ to $\mu = 60$ using the two term sine function $w_D(\mu) = 0.198\sin(0.4159\mu + 2.049) + 0.2418\sin(0.6768\mu + 5.15)$.

$\mu = 0$ to $\mu = 60$—the universe is expanding in some regions and contracting in others [20].

It should be mentioned that the parameter $b$ and $d$ in $K(z)$ and $K'(z)$ respectively, when determined by fitting progressively incremental observed data, show oscillatory behaviour at their respective average value similar to $w_D$. This may be interpreted as if $K$ and $K'$ factors are varying with $\mu$ to effectively correct for the missing effect in their respective Equations (17) and (19). However, they lack any explanation for such behaviour. It remains to be seen if the phenomenological model proposed here can be derived in a fundamental manner.

## 5. Conclusion

The extragalactic redshift has been shown to be due partly to the Doppler effect (expansion of the universe) and partly due to Mach effect by analysing up to date data available from Union2 and NASA/NED data bases. The model resulting in Mach effect yields mass of the observable universe as $\approx 2 \times 10^{53}$ kg. The weight factor determining the two contributions shows an oscillatory behavior against distance modulus when progressively larger set of the database is fitted using the hybrid model comprising both the Doppler effect and the Mach effect. It suggests that the universe is expanding at some radial distances from the observer and contracting at others. However, the phenomenological model for the Mach effect proposed here needs to be related to fundamentals cosmology.

## Acknowledgements

We wish to thank Professor Naser Mostaghel for providing the SNe and Union2 observational data used in his research paper [13], and Professor López-Corredoira for his critical comments on this paper and for providing a copy of his most recent review paper [8]. Acknowledgement is also due to Professor James Peebles who has suggested that the new approach should also be considered for explaining the observed Microwave Background Radiation profile.

## References

[1] Zwicky, F. (1929) On the Red Shift of Spectral Lines through Interstellar Space. *Proceedings of the National Academy of Sciences*, **15**, 773-779. https://doi.org/10.1073/pnas.15.10.773

[2] Geller, M.J. and Peebles, P.J.E. (1972) Test of Expanding Universe Postulate. *Astrophysical Journal*, **174**, 1-5. https://doi.org/10.1086/151462

[3] LaViolette, P.A. (1986) Is the Universe Really Expanding. *Astrophysical Journal*, **301**, 544-553. https://doi.org/10.1086/163922

[4] Ghosh, A. (1997) Velocity Dependent Inertial Induction: A Possible Mechanism for Cosmological Red Shift in a Quasi Static Infinite Universe. *Journal of Astrophysics and Astronomy*, **18**, 449-454. https://doi.org/10.1007/BF02709336

[5] Marosi, L.A. (2014) Hubble Diagram Test of 280 Supernovae Redshift Data. *Journal of Modern Physics*, **5**, 29-33. https://doi.org/10.4236/jmp.2014.51005

[6] Traunmüller, H. (2014) From Magnitudes and Redshifts of Supernovae, Their Light-Curves, and Angular Sizes of Galaxies to a Tenable Cosmology. *Astrophysics and Space Science*, **350**, 755-767. https://doi.org/10.1007/s10509-013-1764-z

[7] Orlov, V.V. and Raikov, A.A. (2016) Cosmological Tests and Evolution of Extragalactic Objects. *Astronomy Reports*, **60**, 477-485. https://doi.org/10.1134/S1063772916030112

[8] López-Corredoira, M. (2017) Test and Problems of the Standard Model in Cosmology. *Foundations of Physics*, **47**, 711-768. https://doi.org/10.1007/s10701-017-0073-8

[9] Carvalho, J.C. (1995) Derivation of the Mass of the Observable Universe. *International Journal of Theoretical Physics*, **34**, 2507-2509. https://doi.org/10.1007/BF00670782

[10] Valev, D. (2014) Estimation of Total Mass and Energy of the Observable Universe. *Physics International*, **5**, 15-20. https://doi.org/10.3844/pisp.2014.15.20

[11] Ostriker, J.P., Peebles, P.J.E. and Yahil, A. (1974) The Size and Mass of the Galaxies, and the Mass of the Universe. *Astrophysical Journal*, **193**, L1-L4. https://doi.org/10.1086/181617

[12] Peacock, J.A. (1999) *Cosmological Physics*, 5-6 (Cambridge).

[13] Mostaghel, N. (2016) A New Solution for the Friedman Equations. *International*

*Journal of Astronomy and Astrophysics*, **6**, 122-134.
https://doi.org/10.4236/ijaa.2016.61010

[14] Amanullah, R., Lidman, C., Rubin, D., Aldering, G., Astier, P., Barbary, K., *et al.* (2010) Spectra and Hubble Space Telescope Light Curves of Six Type Ia Supernovae at 0.511<z<1.12 and the UNION2 Compilation. *The Astrophysical Journal*, **716**, 712-738. https://doi.org/10.1088/0004-637X/716/1/712

[15] Mador, B.F. and Steer, I.P., the NED Team (2017) NED-D: A Master List of Redshift-Independent Extragalactic Distances.
https://ned.ipac.caltech.edu/Library/Distances/

[16] Zitrin, A., Labbé, I., Belli, S., Bouwens, R., Ellis, R.S., Roberts-Borsani, G., *et al.* (2015) Ly$\alpha$ Emission from a Luminous z = 8.68 Galaxy: Implications for Galaxies as Tracers of Cosmic Reionization. *The Astrophysical Journal Letters*, **810**, L12-L17.
https://doi.org/10.1088/2041-8205/810/1/L12

[17] Oesch, P.A., van Dokkum, P.G., Illingworth, G.D., Bouwens, R.J., Momcheva, I., Holden, B., *et al.* (2015) A Spectroscopic Redshift Measurement for a Luminous Lyman Break Galaxy at z = 7.730 Using KECK/MOSFIRE. *The Astrophysical Journal Letters*, **804**, L30-L35. https://doi.org/10.1088/2041-8205/804/2/L30

[18] Finkelstein, S.L., Papovich, C., Dickinson, M., Song, M., Tilvi, V., Koekemoer, A.M., *et al.* (2013) A Galaxy Rapidly Forming Stars 700 Million Years after Big Bang at Redshift 7.51. *Nature*, **502**, 524-527. https://doi.org/10.1038/nature12657

[19] Mortlock, D.J., Warren, S.J., Venemans, B.P., Patel, M., Hewett, P.C., McMahon, R.G., *et al.* (2011) A Luminous Quasar at a Redshift of z = 7.085. *Nature*, **474**, 616-619. https://doi.org/10.1038/nature10159

[20] Narlikar, J.V., Burbidge, G. and Vishwakarma, R.G. (2007) Cosmology and Cosmogony in a Cyclic Universe. *Journal of Astrophysics and Astronomy*, **28**, 67-99.
https://doi.org/10.1007/s12036-007-0007-5